ISSN 1007-9327 (print)
ISSN 2219-2840 (online)

World Journal of *Gastroenterology*

World J Gastroenterol 2024 November 7; 30(41): 4411-4517

Published by Baishideng Publishing Group Inc

World Journal of Gastroenterology

Contents

Weekly Volume 30 Number 41 November 7, 2024

Contents

NAME OF JOURNAL
World Journal of Gastroenterology

ISSN
ISSN 1007-9327 (print) ISSN 2219-2840 (online)

LAUNCH DATE
October 1, 1995

FREQUENCY
Weekly

EDITORS-IN-CHIEF
Andrzej S Tarnawski

EXECUTIVE ASSOCIATE EDITORS-IN-CHIEF
Jian-Gao Fan (Chronic Liver Disease)

EDITORIAL BOARD MEMBERS
http://www.wjgnet.com/1007-9327/editorialboard.htm

PUBLICATION DATE
November 7, 2024

COPYRIGHT
© 2024 Baishideng Publishing Group Inc

PUBLISHING PARTNER
Shanghai Pancreatic Cancer Institute and Pancreatic Cancer Institute, Fudan University
Biliary Tract Disease Institute, Fudan University

INSTRUCTIONS TO AUTHORS
https://www.wjgnet.com/bpg/gerinfo/204

GUIDELINES FOR ETHICS DOCUMENTS
https://www.wjgnet.com/bpg/GerInfo/287

GUIDELINES FOR NON-NATIVE SPEAKERS OF ENGLISH
https://www.wjgnet.com/bpg/gerinfo/240

PUBLICATION ETHICS
https://www.wjgnet.com/bpg/GerInfo/288

PUBLICATION MISCONDUCT
https://www.wjgnet.com/bpg/gerinfo/208

POLICY OF CO-AUTHORS
https://www.wjgnet.com/bpg/GerInfo/310

ARTICLE PROCESSING CHARGE
https://www.wjgnet.com/bpg/gerinfo/242

STEPS FOR SUBMITTING MANUSCRIPTS
https://www.wjgnet.com/bpg/GerInfo/239

ONLINE SUBMISSION
https://www.f6publishing.com

PUBLISHING PARTNER's OFFICIAL WEBSITE
https://www.shca.org.cn
https://www.zs-hospital.sh.cn

E-mail: office@baishideng.com https://www.wjgnet.com

World Journal of Gastroenterology

Submit a Manuscript: https://www.f6publishing.com

World J Gastroenterol 2024 November 7; 30(41): 4449-4460

DOI: 10.3748/wjg.v30.i41.4449

ISSN 1007-9327 (print) ISSN 2219-2840 (online)

ORIGINAL ARTICLE

Basic Study

Amino acid deletions at positions 893 and 894 of cytotoxin-associated gene A protein affect *Helicobacter pylori* gastric epithelial cell interactions

Zhi-Jing Xue, Ya-Nan Gong, Li-Hua He, Lu Sun, Yuan-Hai You, Dong-Jie Fan, Mao-Jun Zhang, Xiao-Mei Yan, Jian-Zhong Zhang

Specialty type: Gastroenterology and hepatology

Provenance and peer review: Unsolicited article; Externally peer reviewed.

Peer-review model: Single blind

Peer-review report's classification

Scientific Quality: Grade B, Grade C

Novelty: Grade B, Grade C

Creativity or Innovation: Grade A, Grade C

Scientific Significance: Grade B, Grade C

P-Reviewer: AlSahman L; Rao RSP

Received: March 12, 2024

Revised: September 29, 2024

Accepted: October 12, 2024

Published online: November 7, 2024

Processing time: 225 Days and 4.1 Hours

Zhi-Jing Xue, Research Center of Translational Medicine, Central Hospital Affiliated to Shandong First Medical University, Jinan 250013, Shandong Province, China

Ya-Nan Gong, Li-Hua He, Lu Sun, Yuan-Hai You, Dong-Jie Fan, Mao-Jun Zhang, Xiao-Mei Yan, Jian-Zhong Zhang, National Key Laboratory of Intelligent Tracking and Forecasting for Infectious Diseases, National Institute for Communicable Disease Control and Prevention, Chinese Center for Disease Control and Prevention, Beijing 102206, China

Corresponding author: Jian-Zhong Zhang, MD, Professor, National Key Laboratory of Intelligent Tracking and Forecasting for Infectious Diseases, National Institute for Communicable Disease Control and Prevention, Chinese Center for Disease Control and Prevention, No. 155 Changbai Road, Changping District, Beijing 102206, China. zhangjianzhong@icdc.cn

Abstract

BACKGROUND

Helicobacter pylori (*H. pylori*) persistently colonizes the human gastric mucosa in more than 50% of the global population, leading to various gastroduodenal diseases ranging from chronic gastritis to gastric carcinoma. Cytotoxin-associated gene A (CagA) protein, an important oncoprotein, has highly polymorphic Glu-Pro-Ile-Tyr-Ala segments at the carboxyl terminus, which play crucial roles in pathogenesis. Our previous study revealed a significant association between amino acid deletions at positions 893 and 894 and gastric cancer.

AIM

To investigate the impact of amino acid deletions at positions 893 and 894 on CagA function.

METHODS

We selected a representative HZT strain from a gastric cancer patient with amino acid deletions at positions 893 and 894. The *cagA* gene was amplified and mutated into *cagA*-NT and *cagA*-NE (sequence characteristics of strains from nongastric cancer patients), cloned and inserted into pAdtrack-CMV, and then transfected into AGS cells. The expression of *cagA* and its mutants was examined using real-time polymerase chain reaction and Western blotting, cell elongation *via* cell

counting, F-actin cytoskeleton visualization using fluorescence staining, and interleukin-8 (IL-8) secretion *via* enzyme-linked immunosorbent assay.

RESULTS

The results revealed that pAdtrack/*cagA* induced a more pronounced hummingbird phenotype than pAdtrack/*cagA*-NT and pAdtrack/*cagA*-NE (40.88 ± 3.10 *vs* 32.50 ± 3.17, $P < 0.001$ and 40.88 ± 3.10 *vs* 32.17 ± 3.00, $P < 0.001$) at 12 hours after transfection. At 24 hours, pAdtrack/*cagA*-NE induced significantly fewer hummingbird phenotypes than pAdtrack/*cagA* and pAdtrack/*cagA*-NT (46.02 ± 2.12 *vs* 53.90 ± 2.10, $P < 0.001$ and 46.02 ± 2.12 *vs* 51.15 ± 3.74, $P < 0.001$). The total amount of F-actin caused by pAdtrack/*cagA* was significantly lower than that caused by pAdtrack/*cagA*-NT and pAdtrack/*cagA*-NE (27.54 ± 17.37 *vs* 41.51 ± 11.90, $P < 0.001$ and 27.54 ± 17.37 *vs* 41.39 ± 14.22, $P < 0.001$) at 12 hours after transfection. Additionally, pAdtrack/*cagA* induced higher IL-8 secretion than pAdtrack/*cagA*-NT and pAdtrack/*cagA*-NE at different times after transfection.

CONCLUSION

Amino acid deletions at positions 893 and 894 enhance CagA pathogenicity, which is crucial for revealing the pathogenic mechanism of CagA and identifying biomarkers of highly pathogenic *H. pylori*.

Key Words: Cytotoxin-associated gene A; Glu-Pro-Ile-Tyr-Ala; Hummingbird phenotype; Interleukin-8; *Helicobacter pylori*

Core Tip: The present study evaluated the impact of amino acid deletions at positions 893 and 894 on cytotoxin-associated gene A (CagA) protein function. Amino acid deletions at positions 893 and 894 enhance the ability of CagA to induce hummingbird cells, cytoskeletal rearrangement, and interleukin-8 secretion. This finding is crucial for elucidating the molecular mechanism of CagA protein pathogenicity and identifying biomarkers of highly pathogenic *Helicobacter pylori*.

Citation: Xue ZJ, Gong YN, He LH, Sun L, You YH, Fan DJ, Zhang MJ, Yan XM, Zhang JZ. Amino acid deletions at positions 893 and 894 of cytotoxin-associated gene A protein affect *Helicobacter pylori* gastric epithelial cell interactions. *World J Gastroenterol* 2024; 30(41): 4449-4460

URL: https://www.wjgnet.com/1007-9327/full/v30/i41/4449.htm

DOI: https://dx.doi.org/10.3748/wjg.v30.i41.4449

INTRODUCTION

For the year 2022, GLOBOCAN 2020 estimated approximately 509421 new cancer cases and 400415 cancer deaths attributed to gastric carcinoma[1]. Among those cases, approximately 352955 and 274691 will be male and 156466 and 125724 female, respectively[1]. Gastric carcinoma is the third most common cause of cancer mortality and the fifth leading cause of malignancy worldwide. In 2020, China had an estimated 478508 new cases, with approximately 373789 deaths[2]. China, with one of the highest mortality and morbidity rates of gastric carcinoma, attributes 90% of cases to *Helicobacter pylori* (*H. pylori*) infection[3].

H. pylori is a microaerophilic, gram-negative bacterium that not only causes chronic gastritis and peptic ulcer disease but also poses a significant risk for the development of gastric adenocarcinoma and mucosal-associated lymphoid tissue lymphoma[4,5]. In 1994, the World Health Organization classified *H. pylori* as a Class I carcinogen, and its eradication is considered a primary preventive measure for gastric cancer. It is recognized as a modifiable risk factor for this malignancy[6]. In addition to environmental factors and host immunity, the difference in the pathogenicity of bacterial virulence factors is the main reason leading to different clinical outcomes[7,8]. *H. pylori* produces a range of pathogenic factors, with cytotoxin-associated gene A (CagA) being one of the most significant virulence factors. It is encoded by the *cagA* gene at the end of the *cag* pathogenicity island, and its molecular weight is approximately 120-145 Ku[9,10]. Research has shown that *cagA*-positive strains cause more severe gastric mucosal injury and inflammation, significantly increasing the risk of gastric cancer[11,12].

The CagA protein can be transferred into gastric epithelial cells through a type IV secretion system[13,14], which is located on the inner surface of the host plasma membrane. This protein is subsequently tyrosine-phosphorylated at the Glu-Pro-Ile-Tyr-Ala (EPIYA) motif at its C-terminus by Src family kinases and Ab1 kinase[15,16]. The C-terminal region of CagA includes four different EPIYA segments, namely, EPIYA-A, EPIYA-B, EPIYA-C, and EPIYA-D, all of which are closely linked to clinical outcomes[17]. *H. pylori* can be categorized into two types on the basis of the different combinations of these four EPIYA segments: East Asian type and Western type[18-20]. CagA can interact with various signaling proteins through four distinct EPIYA segments, either through a phosphorylation-dependent or phosphorylation-independent mechanism, affecting cell proliferation, motility, apoptosis, and the inflammatory response[21,22]. Phosphorylated CagA binds specifically to and activates src-homology-region-2-domain-containing-phosphatase-2 (SHP-2), which in turn triggers activation of the extracellular signal-regulated kinase/mitogen-activated protein kinase (ERK/

MAPK) pathway and the C-terminal src kinase (Csk)[23,24]. The CagA-SHP2 complex, by continuously activating ERK and dephosphorylating focal adhesion kinase, can cause rearrangements in the cytoskeleton, leading to a unique morphological change known as the hummingbird phenotype. This phenotype is characterized by elongated, scattered cells[25-27]. When AGS cells with complete knockout of SHP-2 were infected with *H. pylori*, the number of hummingbird phenotypes was significantly reduced, indicating that SHP-2 plays a crucial role in the morphological changes induced by CagA[28,29]. Furthermore, phosphorylated CagA can directly bind to phosphatidylinositol 3-kinase (PI3K), SHP-1, growth factor receptor-bound protein 7 (Grb7), and Ras-GTPase activator protein 1, leading to abnormal activation of signaling pathways and resulting in cell dysfunction[30]. The aforementioned results were also observed in the interaction of unphosphorylated CagA with certain proteins, including hepatocyte growth factor receptor (c-Met), zonulin-1, and junctional adhesion molecules[31,32]. By disrupting tight junctions and losing cell polarity, the integrity of gastric epithelial cells is compromised, potentially leading to increased cell migration, proliferation, and transformation[33].

H. pylori can activate noncanonical nuclear factor-kappa B (NF-κB) transcription factor through various mechanisms and induce secretion of proinflammatory cytokines, such as interleukin-8 (IL-8)[33,34]. Ritter *et al*[35] reported that the induction of IL-8 was regulated by *cagA*-dependent mechanisms. IL-8 is a neutrophil chemokine that is secreted by gastric epithelial cells. It can induce neutrophil chemotaxis, leading to an inflammatory response in the gastric mucosa. IL-8 plays an important role in the development of gastroduodenal diseases. Higher levels of IL-8 are directly associated with a poorer prognosis and more aggressive gastric carcinoma.

Owing to variations in the number and type of EPIYA segments, CagA displays diversity in terms of geography, structure, and function. Therefore, many studies have investigated the correlation between structural polymorphisms of CagA and clinical outcomes. Our previous study[36] revealed a significant association between the absence of residues 893 and 894 of the CagA protein and strains from gastric cancer patients. In this study, we selected a representative HZT strain containing amino acid deletions at positions 893 and 894 and created various *cagA* mutants to investigate the impact of amino acid deletions at positions 893 and 894 on AGS morphological changes and IL-8 secretion. Our results provide a theoretical basis for further research into the pathogenic mechanism, risk assessment and eradication treatment of *H. pylori* infection.

MATERIALS AND METHODS

Bacterial strains and culture conditions

The HZT strain used in this study was isolated from a gastric mucosa sample of a patient with gastric cancer in Zhejiang Province. The HZT strain was cultured on Karmali agar plates (Oxoid, England) supplemented with 50 mL/L defibrinated sheep blood at 37 °C in a 100 mL/L CO2-humidified atmosphere for 72 hours. The obtained colonies were identified based on catalase, oxidase, and urease tests, negative Gram staining, and bacterial morphology. The *Escherichia coli* (*E. coli*) strain Trans5α (TransGen Biotech, Beijing, China) used for molecular cloning was cultivated on Luria Bertani agar plates (LB, Land Bridge, Beijing, China) supplemented with ampicillin (100 mg/L) as necessary and incubated at 37 °C for 24 hours.

DNA extraction and amplification of the cagA gene

Genomic DNA was extracted from the HZT strain using the QIAamp DNA Mini Kit (QIAGEN, Germany). The concentration and purity of the DNA were measured using a NanoDrop-1000 (Thermo Fisher Scientific, United States). The primers used were designed for amplification of the *cagA* gene, followed by Sanger sequencing. The sequence of the *cagA* forward primer with an endonuclease site of *Kpn*I (New England Biolabs, United States) was 5′-CGCGGTACCATGACTAACGAAACCATCGATCAAACA-3′. The sequence of the *cagA* reverse primer with an endonuclease site of *Xho*I (New England Biolabs, United States) was 5′-CGCCTCGAGTTAAGATTTCTGGAAACCACTTTTTGT-3′. The 2 × Super Pfx MasterMix (CWBIO, Beijing, China) was used to amplify the DNA. The DNA with the designed primers was amplified *via* polymerase chain reaction (PCR) for 30 cycles. The PCR products were analyzed after electrophoresis on a 1% agarose gel with GelStain and sequenced *via* Sanger sequencing (Tsingke, Beijing, China).

Site-directed mutagenesis of the cagA gene

After the *cagA* gene was amplified, sequence alignment analysis revealed that CagA was simultaneously deleted at positions 893 and 894 (26695 was used as a reference strain). Splicing by overlap extension (SOE) PCR was used to insert the asparagine-threonine (NT) codon AACACA and the asparagine-glutamate (NE) codon AACGAA at amino acid deletion positions 893 and 894 of CagA in the HZT strain, respectively, and the *cagA* genes were mutated into *cagA*-NT and *cagA*-NE (sequence characteristics of strains from nongastric cancer patients). The primers used for site-directed mutagenesis of the *cagA* gene are shown in Table 1. C-F and C-R flanking primers were designed with *Kpn*I and *Xho*I endonuclease sites, which were used to amplify the full-length promoter fragment. The two pairs of primers T-F/T-R and E-F/E-R introduced the desired mutations. The flanking primers and mutation primers were matched to amplify mutation sites and promoter fragments. The promoter containing the upstream region of the *cagA* gene was amplified using the C-F and T-R/E-R primers; the downstream region was amplified using the T-F/E-F and C-R primers; and the full-length *cagA* gene was amplified using the C-F and C-R primers. Amplicons containing the upstream region, mutated sequence, and downstream region of the *cagA* gene were fused together *via* SOE PCR. Briefly, in the first SOE PCR, amplicons containing the upstream region of the *cagA* gene were spliced to amplicons containing the mutated *cagA* open reading frame; in the second SOE PCR, the mutated gene was spliced to the downstream region of *cagA*. The products of the two SOE PCRs were purified with the E.Z.N.A.® Gel Extraction Kit (OMEGA, United States) and then spliced together

Table 1 Sequence of primers used for cytotoxin-associated gene A site-directed mutagenesis

Primers	The sequence of primers (5'-3')
C-F	CGC**GAATTC**ATGACTAACGAAACCATCGATCAAACA
C-R	CGC**CTCGAG**TTAAGATTTCTGGAAACCACTTTTTGT
T-F	AATAATGGACTCAAAAAC*AACACA*GAACCCATTTATGCTA
T-R	TAGCATAAATGGGTTC*TGTGTT*GTTTTTGAGTCCATTATT
E-F	AATAATGGACTCAAAAAC*AACGAA*GAACCCATTTATGCTA
E-R	TAGCATAAATGGGTTC*TTCGTT*GTTTTTGAGTCCATTATT

The bold represent the restriction sites, and the italics represent the mutant codons.

in the third step. The final PCR products were gel purified, and site-directed mutations of the *cagA* gene were confirmed *via* DNA sequencing.

Construction of the eukaryotic expression vector of cagA and its mutated genes

The PCR products of *cagA* and its mutated genes were gel purified and cloned and inserted into pMD18-T (Takara, Japan) to construct the vectors pMD18-T/*cagA*, pMD18-T/*cagA*-NT and pMD18-T/*cagA*-NE, followed by sequencing. The recombinant vectors were digested and inserted into *Kpn*I- and *Xho*I-digested pAdtrack-CMV (Nobel Biotech, Shanghai, China). The conditions of the ligation reaction were carried out according to the manufacturer's instructions. The ligated products were subsequently transformed into *E. coli* Trans5α. The positive colonies were screened on LB plates containing ampicillin. The recombinant vectors were extracted with the EndoFree Maxi Plasmid Kit (Tiangen, Beijing, China) and identified *via Kpn*I/*Xho*I double digestion, after which the positive eukaryotic expression vectors were sequenced and termed pAdtrack/*cagA*, pAdtrack/*cagA*-NT, and pAdtrack/*cagA*-NE.

Cell culture and transient transfection

The AGS cell (ATCC CRL1739) was cultured in RPMI-1640 medium (Gibco, Thermo Fisher Scientific, United States) supplemented with 10% fetal bovine serum (FBS) (Gibco, Thermo Fisher Scientific, United States), 100 U/mL of penicillin, and 100 μg/mL of streptomycin (Solarbio, Beijing, China) at 37 °C in a cell culture incubator containing 50 mL/L CO_2. For transient transfection, AGS cells were cultured in 6-well plates at a density of 5 × 10^5 cells per well until they reached approximately 90% confluence. The cells were then transfected with 4 μg of DNA from each plasmid and 4 μL of Lipofectamine 2000 (Invitrogen, Thermo Fisher Scientific, United States) per well. Six hours after transfection, the medium was replaced with antibiotic-free RPMI-1640 medium containing 10% FBS, and the cells were further incubated for 36 hours. We tested five groups of transfections, including the control group (nontransfected cells), the empty plasmid group (transfected with only pAdtrack-CMV), and the experimental groups (transfected with pAdtrack/*cagA*, pAdtrack/*cagA*-NT, and pAdtrack/*cagA*-NE, respectively). All transfections were conducted in triplicate, and the cells were collected at 36 hours for mRNA and protein detection.

RNA extraction and RT-PCR

AGS cells were harvested, and total RNA was extracted using the RNeasy Mini Kit (QIAGEN, Germany). cDNA was synthesized using the QuantiNova Reverse Transcription Kit (QIAGEN, Germany). The forward and reverse primers used for detecting the *cagA* gene were 5'-ATGACTAACGAAACCATCGATCAAACA-3' and 5'-TTAAGATTTCTG-GAAACCACTTTTTGT-3', respectively. The forward and reverse primers used for determining the expression of the internal marker *GAPDH* gene (product size, 258 bp) were 5'AGAAGGCTGGGGCTCATTTG3' and 5'AGGGGCCAT-CCACAGTCTTC3', respectively. The 2 × Super Pfx MasterMix (CWBIO, Beijing, China) was used to amplify the cDNAs. PCR was performed for 30 cycles, and the products were separated on 1% agarose gels, purified, and sequenced.

Western blot analysis

Protein was extracted using the Mammalian Protein Extraction Kit (CWBIO, Beijing, China). Protein quantification was performed *via* a BCA protein quantification kit (TransGen Biotech, Beijing, China). Twenty micrograms of protein were heated at 100 °C for 10 minutes and then loaded for sodium dodecyl sulfate-polyacrylamide gel electrophoresis (SDSPAGE), followed by transfer onto polyvinylidene difluoride (PVDF) membranes (Millipore, United States). The PVDF membranes were blocked with 1 × TBST (CWBIO, Beijing, China) solution containing Difco skim milk for 2 hours and then incubated with primary antibodies against mouse anti-CagA (A-10) (1:200, Santa Cruz, United States) and rabbit anti-GAPDH (1: 2500, Abcam, England) at 4 °C overnight. After the membranes were washed three times with 1 × TBST for 30 minutes, they were incubated with goat anti-mouse m-IgG2a BP-HRP (1: 4000, Santa Cruz, United States) and goat anti-rabbit IgG H&L (HRP) (1: 4000, Abcam, England) for 1 hour, followed by repeated washing as described above. The protein bands were visualized using Western Blot Chemiluminescence HRP Substrate (Takara, Japan) and an ultra-sensitive quantitative fluorescence gel imager (Bio-Rad, United States). The expression of each protein was quantified using ImageJ software (version 1.8.0; Bethesda, United States), normalized to that of GAPDH, and expressed as the fold

change.

Cell elongation assay

AGS cells (1×10^5) were cultured in 6-well plates containing RPMI 1640 medium supplemented with 10% FBS for 24 hours, after which the DNA was transfected into the cells as described above. The morphology of the AGS cells was observed every 6 hours, and 5 random fields were photographed at a magnification of × 100 *via* a Nikon Ci-L inverted microscope (Nikon, Japan). At 12 hours and 24 hours after transfection, the number of hummingbird cells was measured using ImageJ software, and the hummingbird phenotype was defined as cells with needle-like projections that were > 15 μm long and exhibited a characteristic elongated shape.

Fluorescence staining of the F-actin cytoskeleton

AGS cells were cultivated on glass coverslips (WHB, Shanghai, China) within 6-well plates at a concentration of 1×10^5 cells per well and incubated at 37 °C in an atmosphere containing 50 mL/L CO_2 for 24 hours, and the samples were subjected to fluorescence staining at 12 hours and 24 hours after transfection. Briefly, the cell culture medium was carefully aspirated, and the cells were washed twice with PBS. Subsequently, the AGS cells that had adhered to the glass coverslips were first fixed with 4% paraformaldehyde for 10 minutes, followed by permeabilization with 0.5% Triton X-100 for 5 minutes at room temperature. The samples were subsequently treated with FITC phalloidin (Solarbio, Beijing, China) and incubated in the dark at room temperature for 30 minutes. Following staining, the coverslips were removed and inverted onto a slide with mounting medium (with DAPI) (Solarbio, Beijing, China), and the cells were then photographed at a magnification of × 200 using a confocal laser scanning microscope (Nikon, Japan). The F-actin cytoskeleton was quantitatively analyzed by detecting the average fluorescence intensity using ImageJ software. All the experiments were conducted in triplicate.

IL-8 detection

At 6 hours, 12 hours, 24 hours, 36 hours, and 48 hours after transfection, the cell culture supernatants were harvested, centrifuged at 8000 r/minutes for 10 minutes, and then stored at -80 °C until further use. The concentration of IL-8 was quantified using a human IL-8 enzyme-linked immunosorbent assay (ELISA) kit (4A Biotech, Beijing, China) according to the manufacturer's guidelines.

Statistical analysis

Statistical analyses were conducted using SPSS 20.0 (SPSS, Chicago, IL, United States). Each experiment was performed in triplicate and repeated at least three times, and the data are presented as the means ± SDs. Oneway analysis of variance was used for multiple comparisons, and the StudentNewmanKeuls method was used to analyze the mean difference between the two groups. A P value < 0.05 was considered statistically significant.

RESULTS

PCR amplification and site-directed mutagenesis of the cagA gene

The amplified target fragments were approximately 3540 bp in size, which matched the expected size of the target genes (Figure 1A and B). The codons AACACA and AACGAA, representing asparagine-threonine and asparagine-glutamate, respectively, were successfully inserted into the deletion sites at positions 893 and 894 of CagA (Figure 1C), and the corresponding sequences were submitted to the NMDC database under accession numbers NMDCN00011FE to NMDCN00011FG.

Construction and identification of recombinant plasmids

The length of pAdtrack-CMV was 9220 bp; when the target genes were amplified, 6 bp of mutant bases were inserted into the *cagA*-NT and *cagA*-NE genes. Therefore, the lengths of the recombinant plasmids pAdtrack/*cagA*, pAdtrack/*cagA*-NT, and pAdtrack/*cagA*-NE were calculated to be 12760 bp, 12760 bp, and 12760 bp, respectively. After double digestion and electrophoresis, two fragments were produced. Larger DNA fragments were observed at approximately 9000 bp, corresponding to the pAdtrack-CMV fragment (9220 bp), and smaller DNA fragments appeared at approximately 3540 bp, which matched *cagA* and its mutated genes, indicating that the target genes were successfully inserted into pAdtrack-CMV (Figure 1D and E). The sequencing results demonstrated that the recombinant plasmids were successfully constructed, and the mutated bases were successfully inserted into the *cagA* gene.

Transfection and verification by RT-PCR and Western blot analysis

The efficiency of fluorescent transfection was estimated to be > 80% at 36 hours after transfection, as shown in Figure 2. Moreover, RT-PCR and Western blot assays demonstrated successful expression of the *cagA* gene and its mutated variants in AGS cells across the three experimental groups.

Induction of the AGS cell hummingbird phenotype

Compared with the empty plasmid group, the three experimental groups were capable of inducing hummingbird phenotype formation in AGS cells. The hummingbird phenotype was observed to be time dependent, first appearing in AGS cells 6 hours after transfection (Figure 3); by 12-24 hours, it was present in 30%-60% of the cells. Occasionally,

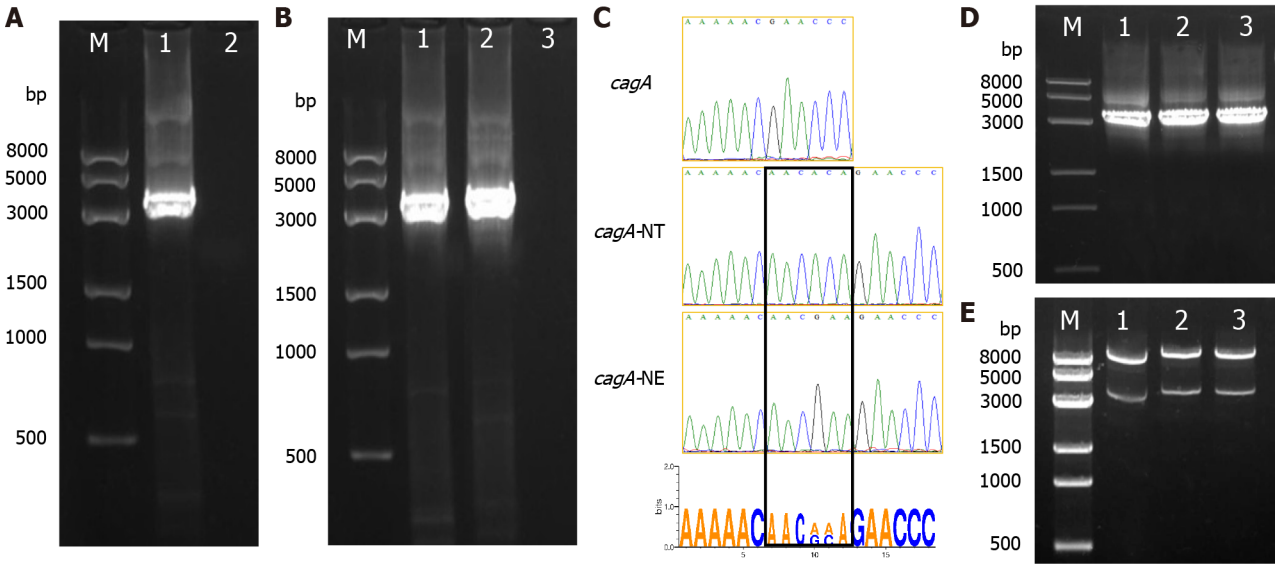

Figure 1 Identification of cytotoxin-associated gene A and its mutated genes. A: The cytotoxin-associated gene A (*cagA*) gene was amplified by polymerase chain reaction (PCR) from the HZT strain. Lane M: DNA marker; lane 1 *cagA* gene; lane 2 Control; B: The mutated gene was amplified by splicing by overlap extension (SOE) PCR. Lane M: DNA marker; lane 1 *cagA*-NT gene; lane 2 *cagA*-NE gene; lane 3 Control; C: Sanger sequencing results; D: The target genes were amplified by PCR from eukaryotic expression recombinant plasmids. Lane M: DL8000 DNA marker; lane 1 pAdtrack/*cagA*; lane 2 pAdtrack/*cagA*-NT; lane 3 pAdtrack/*cagA*-NE; E: Double enzyme identification results. Lane M: DL8000 DNA marker; lane 1 pAdtrack/*cagA*; lane 2 pAdtrack/*cagA*-NT; lane 3 pAdtrack/*cagA*-NE. *cagA*: Cytotoxin-associated gene A.

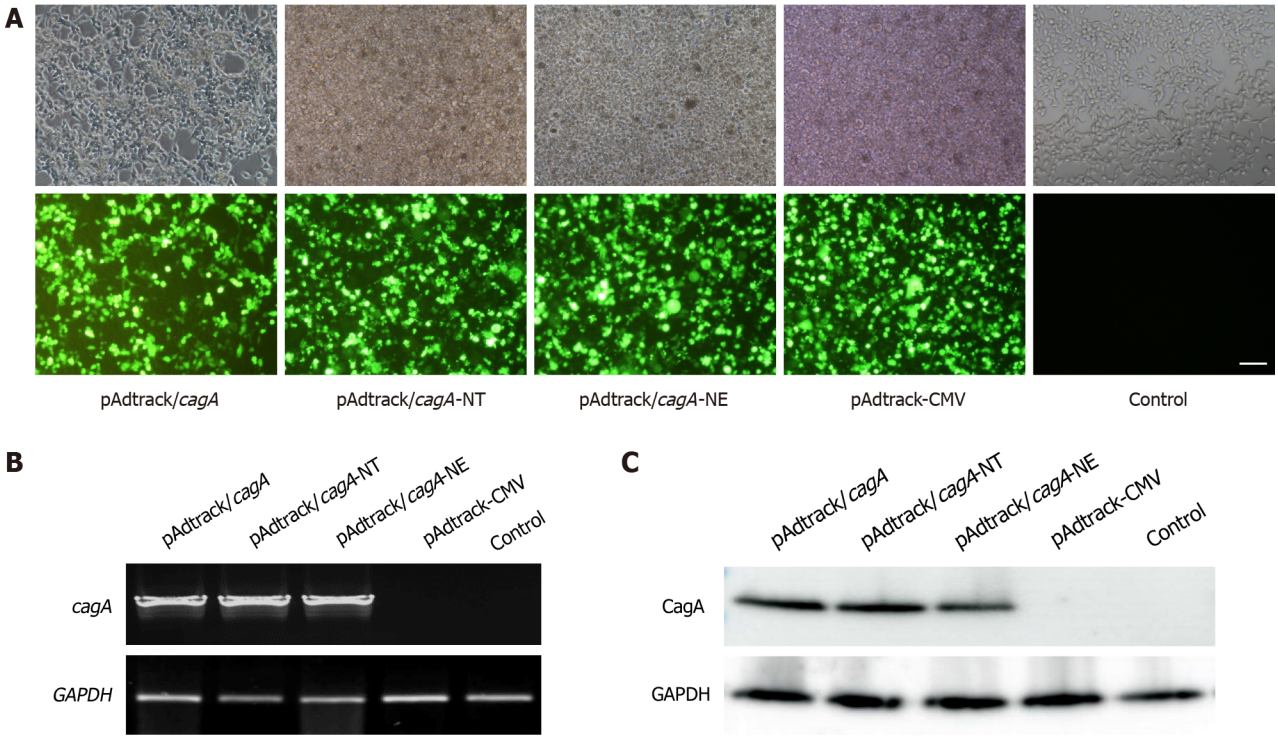

Figure 2 Detection of each plasmid transfection efficiency and expression of each cytotoxin-associated gene A in AGS cells. A: Images under an ordinary light microscope and fluorescence photos after each cytotoxin-associated gene A (*cagA*) transfection into AGS (100 ×). Scale bar = 100 μm; B: The mRNA expression levels in AGS cells; C: The protein levels in AGS cells. CagA proteins were quantified using by Western blot analysis.

elongated AGS cells were also observed in the control group, but these were typically < 10% and exhibited short, needle-like protrusions. Compared with those in the empty plasmid group and the control group, the hummingbird phenotypes induced by the three experimental groups were markedly significantly different at 12 hours and 24 hours after transfection (F = 59.310/236.326, P < 0.001). We found that pAdtrack/*cagA* induced a significantly (P < 0.01) greater number of hummingbird phenotypes than pAdtrack/*cagA*-NT and pAdtrack/*cagA*-NE at 12 hours. Approximately 40% of the AGS cells exhibited a hummingbird phenotype following transfection with pAdtrack/*cagA*, compared with an average of 32%

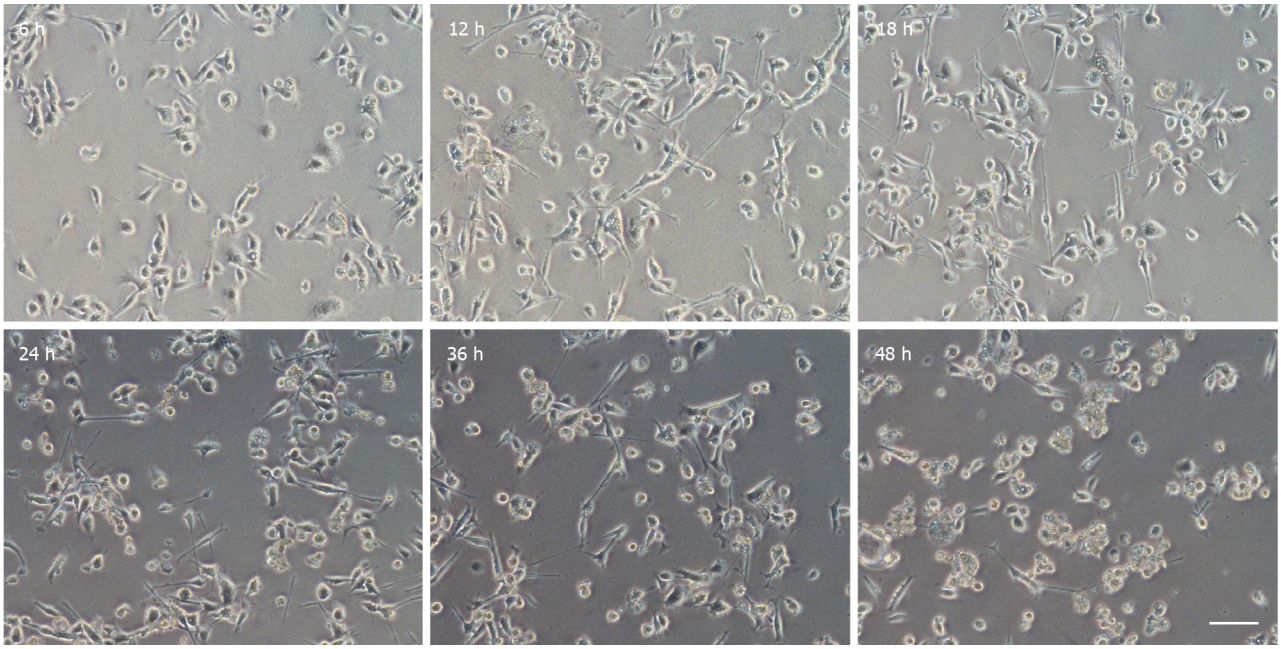

Figure 3 Observation of cell morphology at different times after transfection (100 ×). Representative micrographs of AGS cells transfected with pAdtrack/cytotoxin-associated gene A were shown. Scale bar = 100 μm. *cagA*: Cytotoxin-associated gene A.

of those with pAdtrack/*cagA*-NT and pAdtrack/*cagA*-NE. We also found that pAdtrack/*cagA*-NE induced significantly ($P < 0.05$) fewer hummingbird phenotypes than pAdtrack/*cagA* and pAdtrack/*cagA*-NT at 24 hours. Transfection with pAdtrack/*cagA*-NE resulted in only 46% of the AGS cells showing the hummingbird phenotype, whereas the number of hummingbird cells transfected with pAdtrack/*cagA* and pAdtrack/*cagA*-NT exceeded 50% (Figure 4).

Quantification of the F-actin cytoskeleton with FITC phalloidin staining

To determine whether *cagA* and its mutated genes could trigger actin cytoskeletal rearrangements, the structure and distribution of the F-actin cytoskeleton were measured. Compared to those in the empty plasmid group and the control group, the total amount of F-actin introduced by the three experimental groups was significantly different at 12 hours and 24 hours after transfection ($F = 13.548/21.478$, $P < 0.01$). At 12 hours, the total amount of F-actin caused by pAdtrack/*cagA* was significantly lower than that caused by pAdtrack/*cagA*-NT and pAdtrack/*cagA*-NE ($P < 0.05$). Compared with pAdtrack/*cagA*-NE, pAdtrack/cagA-NE resulted in a statistically significant ($P < 0.05$) increase in the total amount of F-actin at 24 hours. However, there was no significant difference between pAdtrack/*cagA* and pAdtrack/*cagA*-NT (Figure 5). These results suggested that AGS cells transfected with pAdtrack/*cagA* presented major F-actin rearrangement in high abundance at the macrospike protrusions.

Determination of IL-8 secretion

A standard curve of IL-8 was generated according to the manufacturer's instructions, and IL-8 concentrations were quantified *via* ELISA at 6 hours, 12 hours, 24 hours, 36 hours, and 48 hours after transfection. There were notable significant differences in IL-8 secretion among the groups ($P < 0.001$). pAdtrack/*cagA* induced significantly higher levels of IL-8 secretion than pAdtrack/*cagA*-NT and pAdtrack/*cagA*-NE at 6 hours and 24 hours after transfection ($P < 0.05$). At 12 hours after transfection, pAdtrack/*cagA*-NE resulted in significantly lower levels of IL-8 than pAdtrack/*cagA* ($P = 0.006$) and pAdtrack/*cagA*-NT ($P = 0.04$). There were also significant differences among the groups at 36 hours and 48 hours after transfection, with pAdtrack/*cagA* exhibiting significantly greater IL-8 secretion than pAdtrack/*cagA*-NT and pAdtrack/*cagA*-NE ($P < 0.05$). The results are shown in Figure 6.

DISCUSSION

A critical pathogenic factor of *H. pylori*, the CagA protein, has multiple polymorphisms, which play crucial roles in the pathogenic mechanism of *H. pylori*. It has been shown that amino acid polymorphisms flanking the EPIYA-A motif result in functional differences in CagA, but the impact of these polymorphisms on the development and occurrence of gastrointestinal diseases remains unclear[37]. In this study, we investigated the effects of amino acid deletions at positions 893 and 894, adjacent to the EPIYA-A motif, on the functions of CagA. Our findings indicated that these deletions significantly enhanced the ability of CagA to induce a hummingbird phenotype, cytoskeletal rearrangement, and IL-8 secretion. This finding is crucial for elucidating the molecular mechanism of CagA protein pathogenicity and identifying biomarkers of highly pathogenic *H. pylori* in the Chinese population. Translocation and phosphorylation of the CagA protein can lead to cytoskeletal rearrangement and hummingbird phenotype formation. CagA proteins with more EPIYA

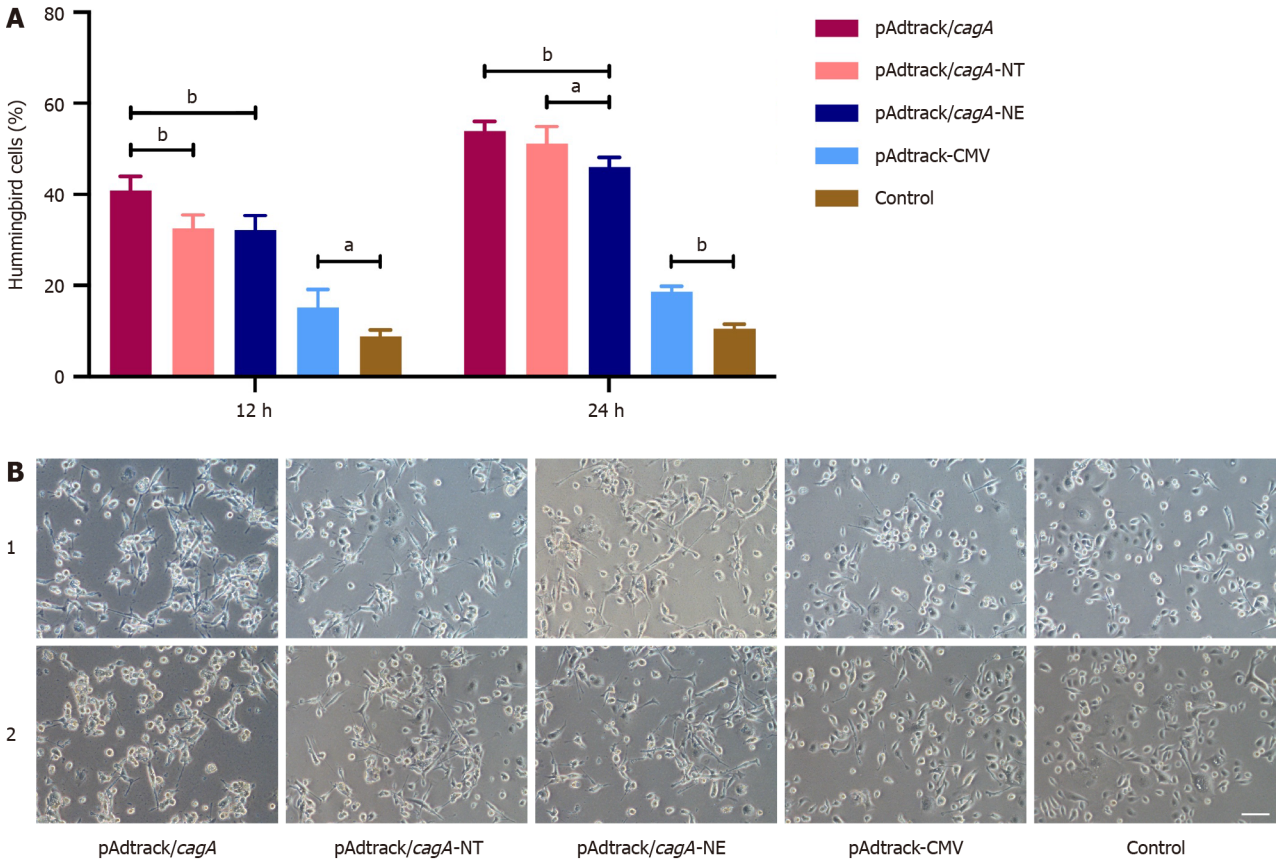

Figure 4 Induction of AGS cells hummingbird phenotype. A: The percentage of hummingbird cells at 12 hours and 24 hours after transfection into AGS. The number of hummingbird cells was quantitated in triplicate in 5 random fields and the results were mean ± SD of three independent experiments. Errors bars represent standard errors of the means. $^{a}P < 0.05$, $^{b}P < 0.01$; B: Representative micrographs of transfected AGS cells as indicated (100 ×). 1 and 2 represented cell morphology at 12 hours and 24 hours after transfection, respectively. Scale bar = 100 μm.

motifs become more phosphorylated, leading to an increase in the number of AGS cells exhibiting the hummingbird phenotype and the length of their cellular protrusions[38]. The phosphorylated EPIYA-C or EPIYA-D segment can specifically bind to and activate SHP-2, a multifunctional signal transduction protein, which is closely related to the regulation of cell life activities such as cell proliferation, differentiation, and death[25,39]. East Asian CagA, which contains the EPIYA-D segment, has a stronger binding ability to SHP-2 and causes more significant cell damage[40]. Western CagA, which contains multiple EPIYA-C segments, has a stronger binding affinity for SHP-2 and induces a hummingbird phenotype more potently than those with fewer EPIYA-C segments[41]. At present, there is no evidence to elucidate the mechanism of gastric cancer caused by CagA-SHP2, but it is worth exploring whether the hummingbird phenotype induced by CagA may be closely related to gastric mucosal carcinogenesis. In addition, the phosphorylated EPIYA-A or EPIYA-B segment can bind to and interact with Csk, which is a negative regulator of Src kinase. Csk phosphorylates the carboxyl terminus of Src kinase, leading to the binding of the phosphorylated residues to the SH2 domain of Src kinase, thus retaining Src kinase in an inhibited state and inhibiting the phosphorylation of EPIYA[42]. This, in turn, prevents the CagA protein, which depends on phosphorylation, from functioning properly. CagA proteins with a greater number of EPIYA-A and EPIYA-B segments can more strongly inhibit Src activity, thereby attenuating tyrosine phosphorylation-dependent CagA activity and reducing cell damage[40]. These findings further suggest that the types of EPIYA-A and EPIYA-B segments may influence their interaction with Csk and consequently affect the phosphorylation capability of CagA. In addition to SHP-2 and Csk, the CagA EPIYA segments can also interact with other signaling factors, such as SHP-1 and PI3K, as well as Crk-I, Crk-II, Grb2, and Grb7, leading to morphological changes and abnormal proliferation[41,42].

Given the hypothesis that amino acid polymorphisms surrounding the EPIYA-A motif affect the virulence and carcinogenic potential of the CagA protein, we assessed the impact of these polymorphisms on the development of morphological changes and the induction of IL-8 secretion in AGS cells. Transfection of AGS cells with the recombinants used in this study demonstrated that both *cagA* and its mutants were capable of inducing the hummingbird phenotype in AGS cells and that the induction of this phenotype was time dependent. By counting hummingbird cells, we observed that pAdtrack/*cagA* induced a significantly greater percentage of cells to exhibit the hummingbird phenotype and induced longer protrusions than pAdtrack/*cagA*-NT and pAdtrack/*cagA*-NE at 12 hours. The number of hummingbird cells induced by pAdtrack/*cagA*-NE was significantly lower than that induced by pAdtrack/*cagA* and pAdtrack/*cagA*-NT at 24 hours. The actin cytoskeleton is a fibrous network that is regulated by the synergistic action of actin-binding proteins[43]. F-actin is a biologically active form of actin that aggregates to form stress fibers and plays crucial roles in cell adhesion, apoptosis, and signal transduction[44]. In the present study, FITC-labeled phalloidin was used to stain F-actin,

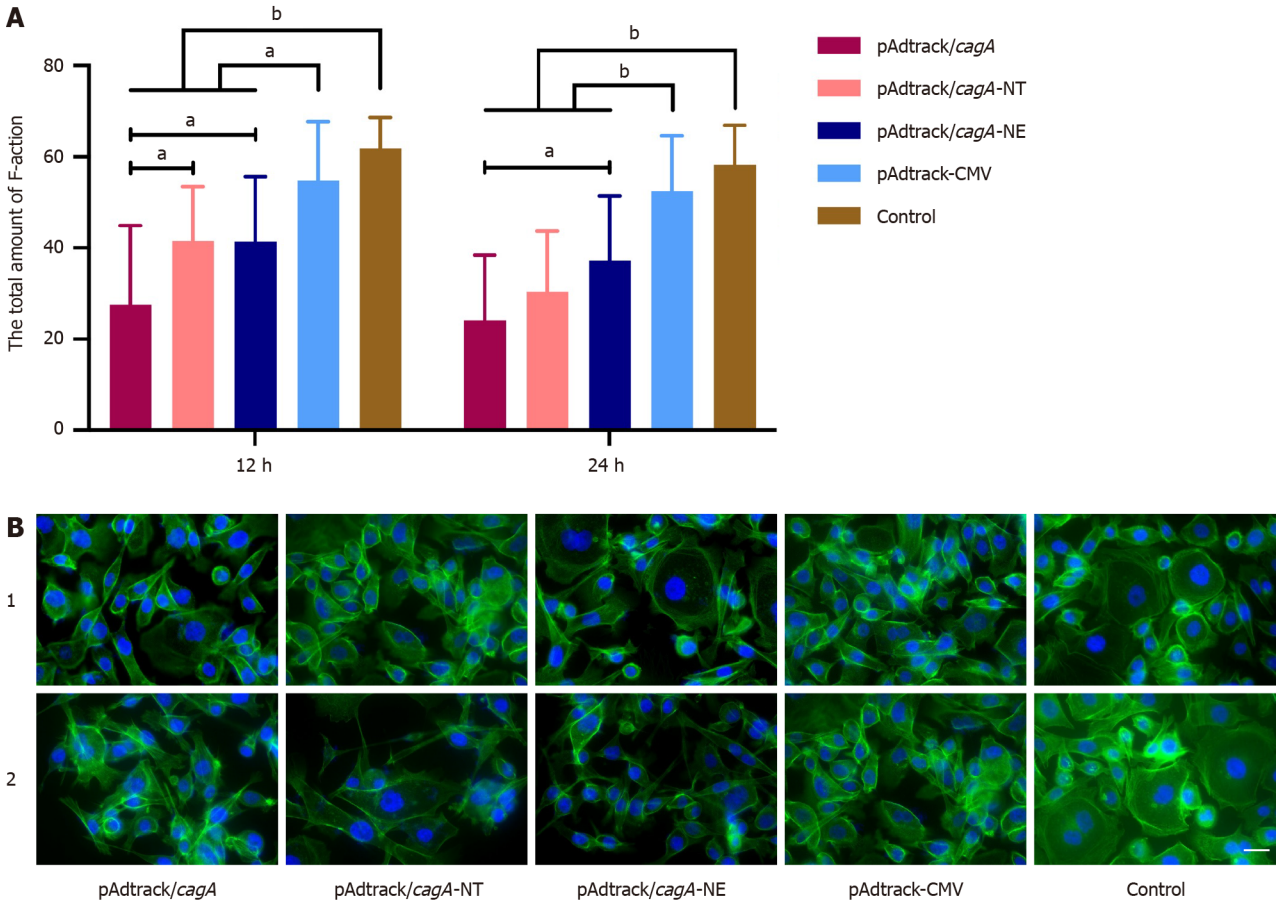

Figure 5 Quantification of the F-actin cytoskeleton with FITC phalloidin stain. A: The average fluorescence intensity of F-actin at 12 hours and 24 hours after transfection. The data were mean ± SD of three independent experiments. Errors bars represented standard errors of the means. $^{a}P < 0.05$, $^{b}P < 0.01$; B: Representative micrographs of F-actin cytoskeleton as indicated (400 ×). AGS cells were labeled for F-actin using FITC phalloidin and the nucleus was stained with DAPI. F-actin was shown in green, and the nucleus was labeled with blue. 1 and 2 represented the F-actin cytoskeleton at 12 hours and 24 hours after transfection, respectively. Scale bar = 25 μm.

and we observed cytoskeletal changes in the host cells, which were characterized by spreading and elongation of the cellular matrix, leading to the formation of needle-like structures filled with F-actin. Our findings revealed that the number of stress fibers significantly increased after transfection with different types of *cagA*. The total amount of F-actin produced by pAdtrack/*cagA* was significantly lower than that produced by pAdtrack/*cagA*-NE ($P < 0.05$) at 12 hours and 24 hours. These findings suggested that the deletion of amino acids 893 and 894 in CagA enhanced its ability to induce the hummingbird phenotype and cytoskeletal rearrangement, with stronger pathogenicity. This phenomenon could be due to the deletion affecting the binding ability of the EPIYA-A segment to Csk, weakening the inhibitory effect of Csk on Src kinase and ultimately enhancing the functional activity of tyrosine phosphorylation-dependent CagA.

The impact of amino acid deletions at positions 893 and 894 on the induction of IL-8 was also examined. Previous studies have shown that the translocation of CagA stimulates the inflammatory response, leading to the activation of NF-κB and the subsequent expression of IL-8[45,46]. IL-8 can promote the proliferation, migration, and survival of endothelial cells, as well as angiogenesis, and enhance the survival of cancer cells[46,47]. Luca *et al*[48] reported that IL-8 can enhance the migration and invasion capabilities of cancer cells. Sugimoto *et al*[49] reported that IL-8 can stimulate angiogenesis and contribute to the development of gastric cancer. Salih *et al*[50] demonstrated that CagA plays a crucial role in inducing IL-8 secretion, and this secretion is dependent on the time of exposure. The EPIYA motif is activated by phosphorylation and negative feedback inhibition, mediating the phosphorylation and activation of multiple downstream protein kinases. Ultimately, it promotes the transcription and expression of IL-8 by regulating the regulatory sequences of the IL-8 gene, such as the promoter and enhancer[51]. The CagA protein can upregulate the expression of inflammatory factors through multiple signaling pathways. The phosphorylated EPIYA-C and EPIYA-D segments can bind to SHP-2 and induce its phosphorylation. By regulating the binding of EGF and EGFR, it can induce the downstream junction protein Grb-2 and ultimately activate NF-κB through the MEK/ERK signaling pathway. Moreover, NF-κB can bind to a specific κB sequence and participate in the inflammatory response[52]. Multiple cellular signaling pathways activate NF-κB, enabling it to enter the nucleus and bind to target gene sites, rapidly inducing the transcription of target genes. This process regulates the expression of genes encoding cytokines, chemokines, and adhesion molecules, leading to the release of inflammatory mediators.

In our study, we observed that IL-8 expression remained stable between 6 hours and 48 hours after transfection, peaking between 24 hours and 48 hours. Notably, pAdtrack/*cagA* induced greater IL-8 secretion compared with

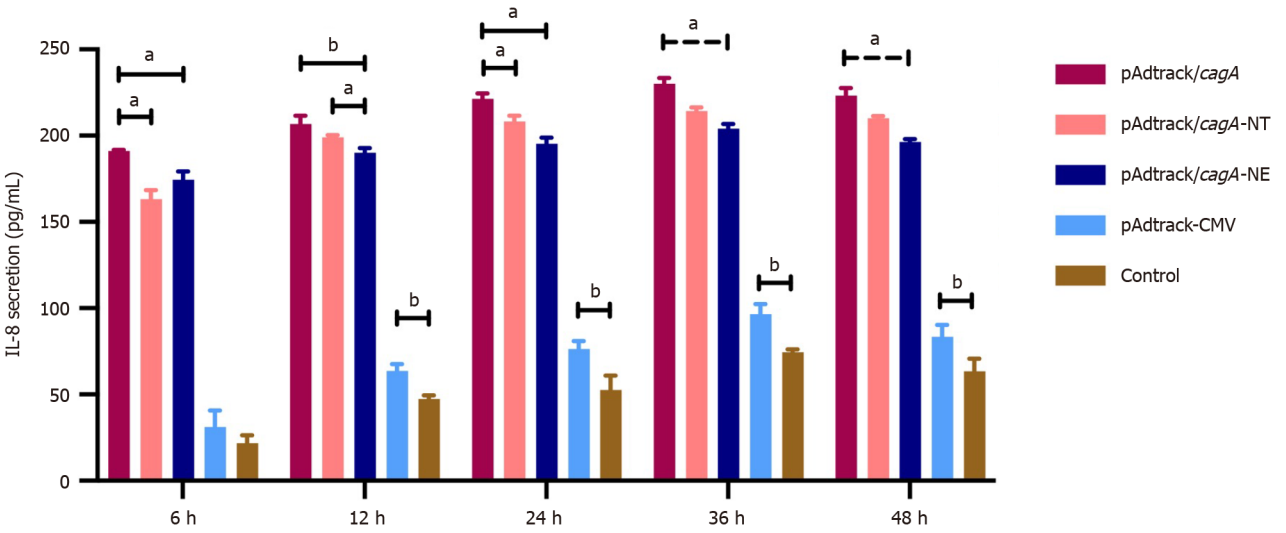

Figure 6 The secretion of interleukin-8 after transfection into AGS cells. The data were mean ± SD of three independent experiments. Errors bars represented standard errors of the means. $^{a}P < 0.05$, $^{b}P < 0.01$. The solid line was the statistical result between the two groups, and the dashed line was the statistical result in multiple groups.

pAdtrack/*cagA*-NT and pAdtrack/*cagA*-NE at different time points after transfection. In addition, at 12 hours, 36 hours, and 48 hours, the level of IL-8 induced by pAdtrack/*cagA*-NT was significantly greater than that induced by pAdtrack/*cagA*-NE. These findings indicated that pAdtrack/*cagA* had the greatest ability to induce IL-8, followed by pAdtrack/*cagA*-NT and pAdtrack/*cagA*-NE. We speculate that the deletion of amino acids at positions 893 and 894 alters the spatial conformation of the CagA protein, weakening its ability to negatively regulate downstream phosphorylation sites, such as EPIYA-C or EPIYA-D, through inhibitory tyrosine motifs. This, in turn, promotes the phosphorylation of EPIYA-C or EPIYA-D, activates downstream protein kinases, and ultimately leads to the expression of the *IL-8* gene.

This study presents the novel finding that amino acid deletions at positions 893 and 894 have a significant effect on CagA function. However, there are certain limitations to this study. The effects of residues 893 and 894 on AGS morphological changes and IL-8 induction were examined only at the molecular and cellular levels in vitro. Further investigations of *H. pylori* infection at the animal and human levels are needed. Moreover, the underlying mechanisms responsible for this effect have not been explored. Future studies should include the construction of site-directed mutants of *H. pylori* strains and the establishment of Mongolian gerbil infection animal models to validate the relationship between the deletion and *H. pylori* pathogenicity, as well as to elucidate the involved specific pathogenic mechanism.

CONCLUSION

The amino acid deletions at positions 893 and 894 flanking the EPIYA-A motif have an impact on CagA function. Specifically, amino acid deletions at positions 893 and 894 significantly enhance the ability of CagA to induce the hummingbird phenotype, cytoskeletal rearrangement, and IL-8 secretion. These findings are crucial for elucidating the molecular mechanism of CagA protein pathogenicity and identifying biomarkers of highly pathogenic *H. pylori*.

FOOTNOTES

Author contributions: Xue ZJ and Zhang JZ designed the research study; Gong YN and He LH constructed the recombinant plasmids; Sun L, You YH, and Fan DJ performed the DNA extraction; Xue ZJ, Zhang MJ, and Yan XM analyzed the data and wrote the manuscript; Zhang JZ reviewed and revised the manuscript; and all authors have read and approved the final manuscript.

Supported by the Shandong Medical and Health Science and Technology Development Plan Project, No. 202202080452.

Institutional review board statement: The study was reviewed and approved by the Institutional Review Board of the National Institute for Communicable Disease Control and Prevention, Chinese Center for Disease Control and Prevention (approval No. ICDC-2013001).

Conflict-of-interest statement: The authors have no conflicts of interest and financial disclosures.

Data sharing statement: No additional data are available.

Country of origin: China

ORCID number: Zhi-Jing Xue 0000-0002-9459-6663; Ya-Nan Gong 0000-0002-4182-1935; Li-Hua He 0000-0002-8391-6035; Yuan-Hai You 0000-0002-4747-660X; Dong-Jie Fan 0000-0002-2468-5783; Jian-Zhong Zhang 0000-0001-7056-8206.

S-Editor: Chen YL
L-Editor: A
P-Editor: Yuan YY

REFERENCES

1 **Xia C**, Dong X, Li H, Cao M, Sun D, He S, Yang F, Yan X, Zhang S, Li N, Chen W. Cancer statistics in China and United States, 2022: profiles, trends, and determinants. *Chin Med J (Engl)* 2022; **135**: 584-590 [PMID: 35143424 DOI: 10.1097/CM9.0000000000002108]
2 **Cao W**, Chen HD, Yu YW, Li N, Chen WQ. Changing profiles of cancer burden worldwide and in China: a secondary analysis of the global cancer statistics 2020. *Chin Med J (Engl)* 2021; **134**: 783-791 [PMID: 33734139 DOI: 10.1097/CM9.0000000000001474]
3 **Bray F**, Ferlay J, Soerjomataram I, Siegel RL, Torre LA, Jemal A. Global cancer statistics 2018: GLOBOCAN estimates of incidence and mortality worldwide for 36 cancers in 185 countries. *CA Cancer J Clin* 2018; **68**: 394-424 [PMID: 30207593 DOI: 10.3322/caac.21492]
4 **Cover TL**, Lacy DB, Ohi MD. The Helicobacter pylori Cag Type IV Secretion System. *Trends Microbiol* 2020; **28**: 682-695 [PMID: 32451226 DOI: 10.1016/j.tim.2020.02.004]
5 **Fujii Y**, Murata-Kamiya N, Hatakeyama M. Helicobacter pylori CagA oncoprotein interacts with SHIP2 to increase its delivery into gastric epithelial cells. *Cancer Sci* 2020; **111**: 1596-1606 [PMID: 32198795 DOI: 10.1111/cas.14391]
6 **Ito N**, Tsujimoto H, Ueno H, Xie Q, Shinomiya N. Helicobacter pylori-Mediated Immunity and Signaling Transduction in Gastric Cancer. *J Clin Med* 2020; **9** [PMID: 33217986 DOI: 10.3390/jcm9113699]
7 **Jeyamani L**, Jayarajan J, Leelakrishnan V, Swaminathan M. CagA and VacA genes of Helicobacter pylori and their clinical relevance. *Indian J Pathol Microbiol* 2018; **61**: 66-69 [PMID: 29567886 DOI: 10.4103/IJPM.IJPM_234_17]
8 **Šterbenc A**, Jarc E, Poljak M, Homan M. Helicobacter pylori virulence genes. *World J Gastroenterol* 2019; **25**: 4870-4884 [PMID: 31543679 DOI: 10.3748/wjg.v25.i33.4870]
9 **Chauhan N**, Tay ACY, Marshall BJ, Jain U. Helicobacter pylori VacA, a distinct toxin exerts diverse functionalities in numerous cells: An overview. *Helicobacter* 2019; **24**: e12544 [PMID: 30324717 DOI: 10.1111/hel.12544]
10 **Lang BJ**, Gorrell RJ, Tafreshi M, Hatakeyama M, Kwok T, Price JT. The Helicobacter pylori cytotoxin CagA is essential for suppressing host heat shock protein expression. *Cell Stress Chaperones* 2016; **21**: 523-533 [PMID: 26928021 DOI: 10.1007/s12192-016-0680-x]
11 **Ansari S**, Yamaoka Y. Helicobacter pylori Virulence Factors Exploiting Gastric Colonization and its Pathogenicity. *Toxins (Basel)* 2019; **11** [PMID: 31752394 DOI: 10.3390/toxins11110677]
12 **Tohidpour A**. CagA-mediated pathogenesis of Helicobacter pylori. *Microb Pathog* 2016; **93**: 44-55 [PMID: 26796299 DOI: 10.1016/j.micpath.2016.01.005]
13 **Boonyanugomol W**, Kongkasame W, Palittapongarnpim P, Baik SC, Jung MH, Shin MK, Kang HL, Lee WK. Genetic variation in the cag pathogenicity island of Helicobacter pylori strains detected from gastroduodenal patients in Thailand. *Braz J Microbiol* 2020; **51**: 1093-1101 [PMID: 32410092 DOI: 10.1007/s42770-020-00292-3]
14 **Merino E**, Flores-Encarnación M, Aguilar-Gutiérrez GR. Functional interaction and structural characteristics of unique components of Helicobacter pylori T4SS. *FEBS J* 2017; **284**: 3540-3549 [PMID: 28470874 DOI: 10.1111/febs.14092]
15 **Khaledi M**, Bagheri N, Validi M, Zamanzad B, Afkhami H, Fathi J, Rahimian G, Gholipour A. Determination of CagA EPIYA motif in Helicobacter pylori strains isolated from patients with digestive disorder. *Heliyon* 2020; **6**: e04971 [PMID: 33005792 DOI: 10.1016/j.heliyon.2020.e04971]
16 **Li Q**, Liu J, Gong Y, Yuan Y. Association of CagA EPIYA-D or EPIYA-C phosphorylation sites with peptic ulcer and gastric cancer risks: A meta-analysis. *Medicine (Baltimore)* 2017; **96**: e6620 [PMID: 28445260 DOI: 10.1097/MD.0000000000006620]
17 **Pachathundikandi SK**, Gutiérrez-Escobar AJ, Tegtmeyer N. Tailor-Made Detection of Individual Phosphorylated and Non-Phosphorylated EPIYA-Motifs of Helicobacter pylori Oncoprotein CagA. *Cancers (Basel)* 2019; **11** [PMID: 31412675 DOI: 10.3390/cancers11081163]
18 **Ansari S**, Yamaoka Y. Helicobacter pylori Virulence Factor Cytotoxin-Associated Gene A (CagA)-Mediated Gastric Pathogenicity. *Int J Mol Sci* 2020; **21** [PMID: 33050101 DOI: 10.3390/ijms21197430]
19 **Tissera K**, Kim MA, Lai J, Angulmaduwa S, Kim A, Merrell DS, Kim JH, Su H, Cha JH. Characterization of East-Asian Helicobacter pylori encoding Western EPIYA-ABC CagA. *J Microbiol* 2022; **60**: 207-214 [PMID: 34757586 DOI: 10.1007/s12275-022-1483-7]
20 **Vianna JS**, Ramis IB, Halicki PC, Gastal OL, Silva RA, Junior JS, Dos Santos DM, Chaves AL, Juliano CR, Jannke HA, da Silva LV Jr, Von Groll A, da Silva PE. Detection of Helicobacter pylori CagA EPIYA in gastric biopsy specimens and its relation to gastric diseases. *Diagn Microbiol Infect Dis* 2015; **83**: 89-92 [PMID: 26144892 DOI: 10.1016/j.diagmicrobio.2015.05.017]
21 **Hayashi T**, Senda M, Morohashi H, Higashi H, Horio M, Kashiba Y, Nagase L, Sasaya D, Shimizu T, Venugopalan N, Kumeta H, Noda NN, Inagaki F, Senda T, Hatakeyama M. Tertiary structure-function analysis reveals the pathogenic signaling potentiation mechanism of Helicobacter pylori oncogenic effector CagA. *Cell Host Microbe* 2012; **12**: 20-33 [PMID: 22817985 DOI: 10.1016/j.chom.2012.05.010]
22 **Müller A**. Multistep activation of the Helicobacter pylori effector CagA. *J Clin Invest* 2012; **122**: 1192-1195 [PMID: 22378039 DOI: 10.1172/JCI61578]
23 **Higashi H**, Nakaya A, Tsutsumi R, Yokoyama K, Fujii Y, Ishikawa S, Higuchi M, Takahashi A, Kurashima Y, Teishikata Y, Tanaka S, Azuma T, Hatakeyama M. Helicobacter pylori CagA induces Ras-independent morphogenetic response through SHP-2 recruitment and activation. *J Biol Chem* 2004; **279**: 17205-17216 [PMID: 14963045 DOI: 10.1074/jbc.M309964200]
24 **Tsutsumi R**, Higashi H, Higuchi M, Okada M, Hatakeyama M. Attenuation of Helicobacter pylori CagA x SHP-2 signaling by interaction between CagA and C-terminal Src kinase. *J Biol Chem* 2003; **278**: 3664-3670 [PMID: 12446738 DOI: 10.1074/jbc.M208155200]

25 **Miyamoto D**, Miyamoto M, Takahashi A, Yomogita Y, Higashi H, Kondo S, Hatakeyama M. Isolation of a distinct class of gain-of-function SHP-2 mutants with oncogenic RAS-like transforming activity from solid tumors. *Oncogene* 2008; **27**: 3508-3515 [PMID: 18223690 DOI: 10.1038/sj.onc.1211019]

26 **Tsutsumi R**, Takahashi A, Azuma T, Higashi H, Hatakeyama M. Focal adhesion kinase is a substrate and downstream effector of SHP-2 complexed with Helicobacter pylori CagA. *Mol Cell Biol* 2006; **26**: 261-276 [PMID: 16354697 DOI: 10.1128/MCB.26.1.261-276.2006]

27 **Zhang J**, Zhang F, Niu R. Functions of Shp2 in cancer. *J Cell Mol Med* 2015; **19**: 2075-2083 [PMID: 26088100 DOI: 10.1111/jcmm.12618]

28 **Coulombe G**, Rivard N. New and Unexpected Biological Functions for the Src-Homology 2 Domain-Containing Phosphatase SHP-2 in the Gastrointestinal Tract. *Cell Mol Gastroenterol Hepatol* 2016; **2**: 11-21 [PMID: 28174704 DOI: 10.1016/j.jcmgh.2015.11.001]

29 **Knorr J**, Backert S, Tegtmeyer N. SHP2-Independent Tyrosine Dephosphorylation of Cortactin and Vinculin during Infection with Helicobacter pylori. *Eur J Microbiol Immunol (Bp)* 2020; **10**: 20-27 [PMID: 32363035 DOI: 10.1556/1886.2020.00001]

30 **Selbach M**, Paul FE, Brandt S, Guye P, Daumke O, Backert S, Dehio C, Mann M. Host cell interactome of tyrosine-phosphorylated bacterial proteins. *Cell Host Microbe* 2009; **5**: 397-403 [PMID: 19380118 DOI: 10.1016/j.chom.2009.03.004]

31 **Churin Y**, Al-Ghoul L, Kepp O, Meyer TF, Birchmeier W, Naumann M. Helicobacter pylori CagA protein targets the c-Met receptor and enhances the motogenic response. *J Cell Biol* 2003; **161**: 249-255 [PMID: 12719469 DOI: 10.1083/jcb.200208039]

32 **Mimuro H**, Suzuki T, Tanaka J, Asahi M, Haas R, Sasakawa C. Grb2 is a key mediator of helicobacter pylori CagA protein activities. *Mol Cell* 2002; **10**: 745-755 [PMID: 12419219 DOI: 10.1016/s1097-2765(02)00681-0]

33 **Viala J**, Chaput C, Boneca IG, Cardona A, Girardin SE, Moran AP, Athman R, Mémet S, Huerre MR, Coyle AJ, DiStefano PS, Sansonetti PJ, Labigne A, Bertin J, Philpott DJ, Ferrero RL. Nod1 responds to peptidoglycan delivered by the Helicobacter pylori cag pathogenicity island. *Nat Immunol* 2004; **5**: 1166-1174 [PMID: 15489856 DOI: 10.1038/ni1131]

34 **Brandt S**, Kwok T, Hartig R, König W, Backert S. NF-kappaB activation and potentiation of proinflammatory responses by the Helicobacter pylori CagA protein. *Proc Natl Acad Sci U S A* 2005; **102**: 9300-9305 [PMID: 15972330 DOI: 10.1073/pnas.0409873102]

35 **Ritter B**, Kilian P, Reboll MR, Resch K, DiStefano JK, Frank R, Beil W, Nourbakhsh M. Differential effects of multiplicity of infection on Helicobacter pylori-induced signaling pathways and interleukin-8 gene transcription. *J Clin Immunol* 2011; **31**: 60-68 [PMID: 20886283 DOI: 10.1007/s10875-010-9467-5]

36 **Xue Z**, You Y, He L, Gong Y, Sun L, Han X, Fan R, Zhai K, Yang Y, Zhang M, Yan X, Zhang J. Diversity of 3' variable region of cagA gene in Helicobacter pylori strains isolated from Chinese population. *Gut Pathog* 2021; **13**: 23 [PMID: 33849660 DOI: 10.1186/s13099-021-00419-3]

37 **Chen CY**, Wang FY, Wan HJ, Jin XX, Wei J, Wang ZK, Liu C, Lu H, Shi H, Li DH, Liu J. Amino acid polymorphisms flanking the EPIYA-A motif of Helicobacter pylori CagA C-terminal region is associated with gastric cancer in east China: experience from a single center. *J Dig Dis* 2013; **14**: 358-365 [PMID: 23517408 DOI: 10.1111/1751-2980.12056]

38 **Vaziri F**, Peerayeh SN, Alebouyeh M, Maghsoudi N, Azimzadeh P, Siadat SD, Zali MR. Novel effects of Helicobacter pylori CagA on key genes of gastric cancer signal transduction: a comparative transfection study. *Pathog Dis* 2015; **73** [PMID: 25743471 DOI: 10.1093/femspd/ftu021]

39 **Saito Y**, Murata-Kamiya N, Hirayama T, Ohba Y, Hatakeyama M. Conversion of Helicobacter pylori CagA from senescence inducer to oncogenic driver through polarity-dependent regulation of p21. *J Exp Med* 2010; **207**: 2157-2174 [PMID: 20855497 DOI: 10.1084/jem.20100602]

40 **Naito M**, Yamazaki T, Tsutsumi R, Higashi H, Onoe K, Yamazaki S, Azuma T, Hatakeyama M. Influence of EPIYA-repeat polymorphism on the phosphorylation-dependent biological activity of Helicobacter pylori CagA. *Gastroenterology* 2006; **130**: 1181-1190 [PMID: 16618412 DOI: 10.1053/j.gastro.2005.12.038]

41 **Hatakeyama M**. Helicobacter pylori CagA and gastric cancer: a paradigm for hit-and-run carcinogenesis. *Cell Host Microbe* 2014; **15**: 306-316 [PMID: 24629337 DOI: 10.1016/j.chom.2014.02.008]

42 **Backert S**, Tegtmeyer N, Selbach M. The versatility of Helicobacter pylori CagA effector protein functions: The master key hypothesis. *Helicobacter* 2010; **15**: 163-176 [PMID: 20557357 DOI: 10.1111/j.1523-5378.2010.00759.x]

43 **Singer II**, Kazazis DM, Kawka DW, Rupp EA, Bayne EK. Extracellular matrix-cytoskeletal interactions in rheumatoid arthritis. I. Immunoelectron microscopic analysis of the fibronexus at the adhesive surface of normal porcine type B synoviocytes in vitro. *Arthritis Rheum* 1985; **28**: 1105-1116 [PMID: 3902032 DOI: 10.1002/art.1780281005]

44 **Connolly M**, Veale DJ, Fearon U. Acute serum amyloid A regulates cytoskeletal rearrangement, cell matrix interactions and promotes cell migration in rheumatoid arthritis. *Ann Rheum Dis* 2011; **70**: 1296-1303 [PMID: 21482536 DOI: 10.1136/ard.2010.142240]

45 **Lamb A**, Yang XD, Tsang YH, Li JD, Higashi H, Hatakeyama M, Peek RM, Blanke SR, Chen LF. Helicobacter pylori CagA activates NF-kappaB by targeting TAK1 for TRAF6-mediated Lys 63 ubiquitination. *EMBO Rep* 2009; **10**: 1242-1249 [PMID: 19820695 DOI: 10.1038/embor.2009.210]

46 **Xie K**. Interleukin-8 and human cancer biology. *Cytokine Growth Factor Rev* 2001; **12**: 375-391 [PMID: 11544106 DOI: 10.1016/s1359-6101(01)00016-8]

47 **Kim JH**. Interleukin-8 in the Tumor Immune Niche: Lessons from Comparative Oncology. *Adv Exp Med Biol* 2020; **1240**: 25-33 [PMID: 32060885 DOI: 10.1007/978-3-030-38315-2_2]

48 **Luca M**, Huang S, Gershenwald JE, Singh RK, Reich R, Bar-Eli M. Expression of interleukin-8 by human melanoma cells up-regulates MMP-2 activity and increases tumor growth and metastasis. *Am J Pathol* 1997; **151**: 1105-1113 [PMID: 9327744]

49 **Sugimoto M**, Yamaoka Y, Furuta T. Influence of interleukin polymorphisms on development of gastric cancer and peptic ulcer. *World J Gastroenterol* 2010; **16**: 1188-1200 [PMID: 20222161 DOI: 10.3748/wjg.v16.i10.1188]

50 **Salih BA**, Guner A, Karademir A, Uslu M, Ovali MA, Yazici D, Bolek BK, Arikan S. Evaluation of the effect of cagPAI genes of Helicobacter pylori on AGS epithelial cell morphology and IL-8 secretion. *Antonie Van Leeuwenhoek* 2014; **105**: 179-189 [PMID: 24170115 DOI: 10.1007/s10482-013-0064-5]

51 **O'Hara AM**, Bhattacharyya A, Mifflin RC, Smith MF, Ryan KA, Scott KG, Naganuma M, Casola A, Izumi T, Mitra S, Ernst PB, Crowe SE. Interleukin-8 induction by Helicobacter pylori in gastric epithelial cells is dependent on apurinic/apyrimidinic endonuclease-1/redox factor-1. *J Immunol* 2006; **177**: 7990-7999 [PMID: 17114472 DOI: 10.4049/jimmunol.177.11.7990]

52 **Karin M**. Nuclear factor-kappaB in cancer development and progression. *Nature* 2006; **441**: 431-436 [PMID: 16724054 DOI: 10.1038/nature04870]

Published by **Baishideng Publishing Group Inc**
7041 Koll Center Parkway, Suite 160, Pleasanton, CA 94566, USA
Telephone: +1-925-3991568
E-mail: office@baishideng.com
Help Desk: https://www.f6publishing.com/helpdesk
https://www.wjgnet.com